NASA TECHNICAL NOTE

NASA TN D-5045

C. 1

NASA TN D-5045

TUFT-GRID SURVEYS AT LOW SPEEDS FOR DELTA WINGS

by John D. Bird

Langley Research Center
Langley Station, Hampton, Va.

NATIONAL AERONAUTICS AND SPACE ADMINISTRATION • WASHINGTON, D. C. • FEBRUARY 1969

TUFT-GRID SURVEYS AT LOW SPEEDS FOR DELTA WINGS

By John D. Bird

Langley Research Center
Langley Station, Hampton, Va.

NATIONAL AERONAUTICS AND SPACE ADMINISTRATION

For sale by the Clearinghouse for Federal Scientific and Technical Information
Springfield, Virginia 22151 – CFSTI price $3.00

TUFT-GRID SURVEYS AT LOW SPEEDS FOR DELTA WINGS

By John D. Bird
Langley Research Center

SUMMARY

Tuft-grid surveys were made along the chord and in the near wake of 60°, 75°, 82.5°, and 86.5° delta wings at low speeds in the Langley stability tunnel to show the nature of the flow in the vicinity of such wing planforms. The results are presented without a detailed discussion in that the photographs of the flow patterns are felt to be largely self-explanatory. An unusual wake pattern which gave evidence of three asymmetrically arranged trailing vortices was obtained for the 86.5° delta wing at an angle of attack of 25° and zero sideslip.

INTRODUCTION

Trends in the aerodynamic design of supersonic aircraft have been toward the use of delta and other wing planforms with swept leading edges and low aspect ratios. These planforms have substantially different aerodynamic characteristics at the higher values of angle of attack than the rather straight high-aspect-ratio wings used for subsonic flight. Because of these differences and their implications, a good understanding of the flow fields existing in the vicinity of and downstream of these lifting surfaces is important in the design of aircraft and missiles and in the development of appropriate theoretical treatments.

References 1 to 7 are analytical treatments of the aerodynamics of delta wings and references 8 to 14 are representative of experimental investigations that contribute to the understanding of the flow about delta wings.

The present investigation was made to obtain a general view of the flow field about delta wings having 60°, 75°, 82.5°, and 86.5° leading-edge sweep at low speed by use of the tuft-grid technique employed in references 8, 9, and 15. The tuft-grid technique involves photographing from far downstream, the action of a great number of tufts of uniform length mounted on a screen which is placed in the wake of a wing or other aerodynamic form. (See fig. 1.) This operation yields an approximate vector plot of the flow field in a plane normal to the airstream at a station in the wake of an aerodynamic surface. The vertical and horizontal projections of each tuft are representative of the downwash and sidewash angles of the flow.

One particular objective of this investigation was to employ the tuft grid to obtain a pictorial view of the development of circulation along the chord of delta wings. This usage involves cutting a horizontal slit in the tuft grid so that the grid may be located at various chordwise positions on the wing, rather than in the wake. This application is similar to that of reference 15.

The results of this investigation are presented without a detailed discussion because the photographs of the flow patterns are felt to be largely self-explanatory.

SYMBOLS

C_L lift coefficient

c_r root chord of wing

x_r station on wing measured from leading edge of root chord, positive aft

α angle of attack, deg

$\Delta\alpha$ jet boundary correction to α

β angle of sideslip, deg

APPARATUS, MODELS, AND TESTS

The tuft grid employed in this investigation consisted of a rectangular grid of fine wires (0.012-inch-diameter (0.30 mm)) of 1-inch (25.4-mm) mesh supported at the periphery by a tubular framework with 3-inch-long (76.2-mm) woolen tufts attached at the intersections of the wires. The tufted area of the grid was 50 inches wide (1.27 m) and 32 inches high (0.81 m). A preloading system consisting of a spring mounted between one end of each wire and the frame was used to maintain a 1.5-pound (6.67-N) tension in each wire. Each intersection of a vertical and horizontal wire was soldered so that relative movement between wires would be eliminated.

The tufts were of 4-ply wool baby yarn and were attached to the grid with strong thread. A small loop of thread was provided at the attaching point in order to permit the tuft to move freely in all directions. The downstream end of each tuft was tied with thread to prevent the strands of wool from unraveling. The frame was fashioned from thin-wall streamline tubing having a 0.75-inch (19.05-mm) chord. Mounting brackets were located at each of the four corners for attaching the frame to the supporting system

used in the tunnel. A close-range photograph showing the wires and tufts of a similar but larger tuft grid mounted in the test section of the Langley 300-MPH 7- by 10-foot tunnel is shown in figure 2.

Tunnel Setup

A cutaway view of a section of a wind tunnel showing the general location of the camera, the tuft grid, and the model is presented in figure 1(a). The camera can only record the projections of the tufts and model in a plane perpendicular to the free stream. Still- or motion-picture cameras may be used for photographing the grid. For these tests a sequence camera with a 20-inch (0.50-m) focal-length lens was employed. The camera was placed 60 feet (18.25 m) downstream of the tuft grid for all tests in order to minimize parallax.

Photographic Interpretation

In the relatively undisturbed regions of flow, the tufts appear as short lines or dots; and in the disturbed regions, as longer lines. The vertical and horizontal projections of each tuft, together with the tuft length and parallax correction, determine the downwash and sidewash angles of the flow at a given location. (See fig. 1(b).) A practical limit of accuracy of the tuft grid employed in this investigation is believed to be $\pm 1/2^{\circ}$ for an individual tuft for regions of reasonably steady flow. Parallax amounts to about 2° at the corners of the grid. At a specific point, however, actual determination of the change in downwash caused by some small model modification, such as filleting, could be better accomplished by the use of a pitot-yaw tube.

Models

Four wings whose pertinent geometric characteristics are given in table I were tested for this investigation. They all had delta-wing planforms and "flat-plate" airfoil sections. The flat-plate airfoil section was obtained by constructing the wings of 3/4-inch (19.05-mm) plywood and rounding the leading edge and cutting an 8° bevel on the trailing edge.

Tests

All the tests were conducted in the 6- by 6-foot (1.83- by 1.83-m) test section of the Langley stability tunnel at a dynamic pressure of 25 pounds per square foot (about 1200 N/m^2), which corresponds to a velocity of about 100 miles per hour (45 m/sec) and to a Reynolds number of 2 770 000 based on a 0.3-m root chord.

Tuft-grid surveys were made for the conditions given in table II, and are given in figures 3 to 22 as indicated in the table. Surveys were made along the chord at various stations for the 60° and 75° delta wings at two angles of attack, as well as in the wake for

certain angles of sideslip and angles of attack. Surveys were only made in the wake for the 82.5° and 86.5° delta wings.

The angles of attack quoted here are the geometric angles of attack of the models in the tunnel. They should be increased by the following amounts to account for the jet boundary effect and to obtain a more correct aerodynamic angle of attack. The lift coefficients are not given herein.

Wing sweep, deg	$\Delta\alpha/C_L$
60	0.90
75	.54
82.5	.26
86.5	.12

RESULTS AND DISCUSSION

Surveys at Various Chord Positions

An examination of figures 3, 4, 7, and 8 shows the characteristic shedding of the vortex sheet along the leading edges of the 60° and 75° delta wings. This shed vortex sheet which results from the separation of the flow around the wing leading edge moves upward and inboard over the upper surface of the wing and rolls up to form two stable vortex cores. This phenomenon is described in references 10 to 14. Figure 23 is a line drawing showing the flow separation tangent to the leading edge and the subsequent development of the vortex system above the surface of a delta wing. This flow separation is similar to that which occurs at the trailing edge of wings. Figure 8 shows the development of this vortex system across the chord of the wing very clearly. Near the wing apex, the vortex system is small whereas at the trailing edge the vortex system is large and very strong. The separation of the flow more or less tangent to the spanwise extremity of the wing followed by a sharp turn toward the upper surface may be seen at the various chordwise stations also. The coarseness of the tuft grid and clutter of the tufts is such that a secondary vortex near each leading edge which is mentioned in some of the reference material is not evident in these photographs. Enlarged photographs of the survey made on the 75° delta wing at an angle of attack of 20° are shown for the 0.70, 0.83, 0.92, and 1.00 x_r/c_r stations in figures 11 to 14. These latter figures make the passage of the vorticity from the leading edge to the upper surface of the wing more evident.

Photographs of the flow in the wake of the 60° and 75° wings are shown for a range of angle of attack at zero sideslip and at an angle of attack of 20° for a range of sideslip in figures 5, 6, 9, and 10. Figures 6 and 10 show the development of an asymmetric character to the trailing vortex system as sideslip is increased.

Surveys Behind 82.5° and 86.5° Wings

Figures 15, 16, 17, and 18 are tuft-grid surveys behind the 82.5° and 86.5° wings through the angle-of-attack and sideslip ranges. Figure 17 for the 86.5° wing shows an interesting development of an asymmetrical trailing-vortex system at zero sideslip beginning at an angle of attack of 15° and extending to an angle of attack of 30°. The vortex pattern alternates in position, similar to the orientations for a Karman vortex street, as the angle of attack is increased in 5° increments. Such vortex patterns can be found in the wake of slender bodies of revolution (ref. 16). At angles of attack of 25° and 30°, there is evidence of three trailing vortices rather than two. The condition was steady at a given angle of attack and did not alternate in time. This condition was not evident for the 82.5° wing at zero sideslip (fig. 15) although a slight tendency toward an unsymmetrical vortex pair was evident at an angle of attack of 30°. A strongly unsymmetrical vortex pair was evident for the 86.5° wing with sideslip for an angle of attack of 25°. (See fig. 18.) The vortex on the left at an angle of sideslip of 15° was located behind the apex of the delta wing, whereas the vortex at the right was located near the right wing tip. It is interesting to note that the cross-flow Reynolds number for the 86.5° wing at an angle of attack of 20° is near the transition Reynolds number of 320 000 for the flow of air on a flat plate. (See ref. 17.)

Figures 19, 20, 21, and 22 are enlarged photographs of the surveys behind the 60°, 75°, 82.5°, and 86.5° wings at zero sideslip and an angle of attack of 25°. The change in the character of the trailing-vortex system as the wing leading-edge sweep is increased is more evident in these photographs.

CONCLUDING REMARKS

Tuft-grid surveys were made along the chord and in the near wake of 60° and 75° delta wings and in the wake of 82.5° and 86.5° delta wings at low speeds to show the nature of the flow in the vicinity of such wing planforms. The results are presented without a detailed discussion because the photographs of the flow patterns are felt to be largely self-explanatory. An unusual wake flow pattern which gave evidence of three asymmetrically arranged trailing vortices was obtained for the 86.5° delta wing at an angle of attack of 25° and zero sideslip.

Langley Research Center,
National Aeronautics and Space Administration,
Langley Station, Hampton, Va., November 27, 1968,
126-13-02-27-23.

REFERENCES

1. Brown, C. E.; and Michael, W. H., Jr.: Effect of Leading-Edge Separation on the Lift of a Delta Wing. J. Aeron. Sci., vol. 21, no. 10, Oct. 1954, pp. 690-694, 706.

2. Mangler, K. W.; and Smith, J. H. B.: A Theory of the Flow Past a Slender Delta Wing With Leading Edge Separation. Proc. Roy. Soc., ser. A, vol. 251, no. 1265, May 26, 1959, pp. 200-217.

3. Smith, J. H. B.: Improved Calculations of Leading-Edge Separation From Slender Delta Wings. Tech. Rep. 66070, Brit. R.A.E., Mar. 1966.

4. Hall, M. G.: A Theory for the Core of a Leading Edge Vortex. Rep. No. Aero. 2644, Brit. R.A.E., Dec. 1960.

5. Legendre, Robert: Écoulement au Voisinage de la Pointe avant d' une Aile à forte flèche aux Incidences moyennes. La Recherche Aéronautique (O.N.E.R.A.), No. 30, Nov.-Dec. 1952, pp. 3-8; No. 31, Jan.-Feb. 1953, pp. 3-6.

6. Polhamus, Edward C.: A Concept of the Vortex Lift of Sharp-Edge Delta Wings Based on a Leading-Edge-Suction Analogy. NASA TN D-3767, 1966.

7. Polhamus, Edward C.: Application of the Leading-Edge Suction Analogy of Vortex Lift to the Drag Due to Lift of Sharp-Edge Delta Wings. NASA TN D-4739, 1968.

8. Bird, John D.; and Riley, Donald R.: Some Experiments on Visualization of Flow Fields Behind Low-Aspect-Ratio Wings by Means of a Tuft Grid. NACA TN 2674, 1952.

9. Bird, John D.: Visualization of Flow Fields by Use of a Tuft Grid Technique. J. Aeron. Sci., vol. 19, no. 7, July 1952, pp. 481-485.

10. Örnberg, Torsten: A Note on the Flow Around Delta Wings. KTH-Aero TN 38, Div. Aeron., Roy. Inst. Technol. (Stockholm), 1954.

11. Gould, R. W. F.; and Cowdrey, C. F.: High Reynolds Number Tests on a 70° L. E. Sweepback Delta Wing and Body (H.P. 100) in the Compressed Air Tunnel. C.P. No. 387, Brit. A.R.C., 1958.

12. Lee, G. H.: Note on the Flow Around Delta Wings With Sharp Leading Edges. R. & M. No. 3070, Brit. A.R.C., 1958.

13. Rainbird, W. J.; Crabbe, R. S.; Peake, D. J.; and Meyer, R. F.: Some Examples of Separation in Three-Dimensional Flows. Can. Aeron. Space J., vol. 12, no. 10, Dec. 1966, pp. 409-423.

14. Werlé, H.: Essais De Soufflage au Tunnel Hydrodynamique a Visualisation. O.N.E.R.A. Note Tech. No. 61, 1960.

15. Michael, William H., Jr.: Flow Studies in the Vicinity of a Modified Flat-Plate Rectangular Wing of Aspect Ratio 0.25. NACA TN 2790, 1952.

16. Letko, William: A Low-Speed Experimental Study of the Directional Characteristics of a Sharp-Nosed Fuselage Through a Large Angle-of-Attack Range at Zero Angle of Sideslip. NACA TN 2911, 1953.

17. Schlichting, Hermann (J. Kestin, trans.): Boundary-Layer Theory. Sixth ed., McGraw-Hill Book Co., 1968.

TABLE I.- GEOMETRIC CHARACTERISTICS OF WINGS TESTED

Sweep, deg	Aspect ratio	Wing span, in.	Root chord, in.
60.0	2.31	36.0	31.2
75.0	1.07	18.5	34.5
82.5	.53	10.3	39.0
86.5	.24	5.5	45.0

TABLE II.- SUMMARY OF DATA FIGURES

Figure	Wing, deg	α, deg	β, deg	Tuft-grid position, x_r/c_r
3	60	10	0	-0.03, 0.20, 0.40, 0.70, 0.88, 1.00, 1.10, 1.20
4	60	20	0	-0.03, 0.20, 0.40, 0.70, 0.88, 1.00, 1.10, 1.20
5	60	0, 5, 10, 15, 20, 25, 30	0	1.20
6	60	20	0, 5, 10, 15	1.20
7	75	10	0	-0.11, 0.25, 0.37, 0.70, 0.83, 0.92, 1.00, 1.10
8	75	20	0	-0.11, 0.25, 0.37, 0.70, 0.83, 0.92, 1.00, 1.10
9	75	0, 5, 10, 15, 20, 25	0	1.20
10	75	20	0, 5, 10, 15	1.20
11	75	20	0	.70
12	75	20	0	.83
13	75	20	0	.92
14	75	20	0	1.00
15	82.5	0, 5, 15, 20, 25, 30	0	1.20
16	82.5	25	0, 5, 10, 15	1.20
17	86.5	0, 5, 10, 15, 20, 25, 30	0	1.20
18	86.5	25	0, 5, 10, 15	1.20
19	60	25	0	1.20
20	75	25	0	1.20
21	82.5	25	0	1.20
22	86.5	25	0	1.20

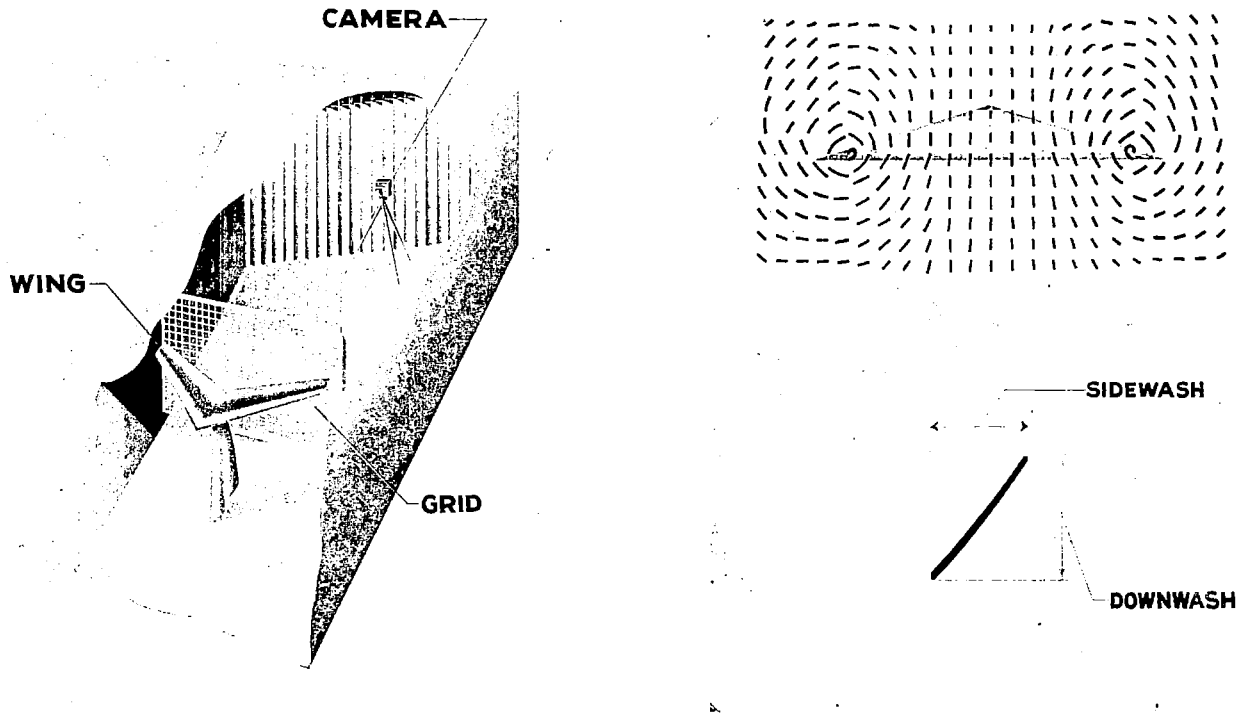

(a) Setup for flow surveys with tuft grid.

(b) Typical flow pattern for triangular wing.

Figure 1.- General arrangement of tuft-grid setup and interpretation of results as sidewash and downwash.

L-70553

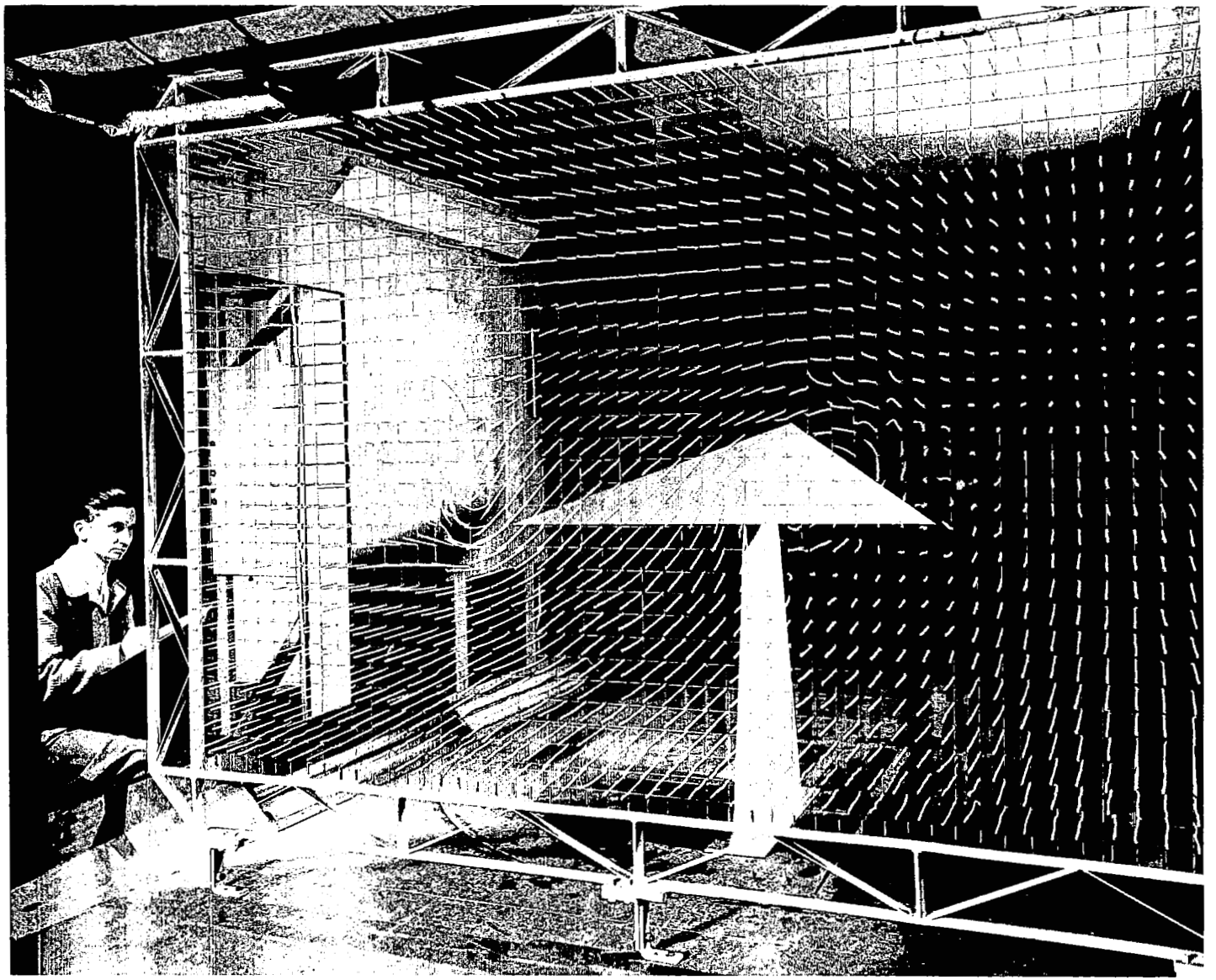

Figure 2.- A tuft grid mounted in the Langley 300-MPH 7- by 10-foot tunnel. L-70315

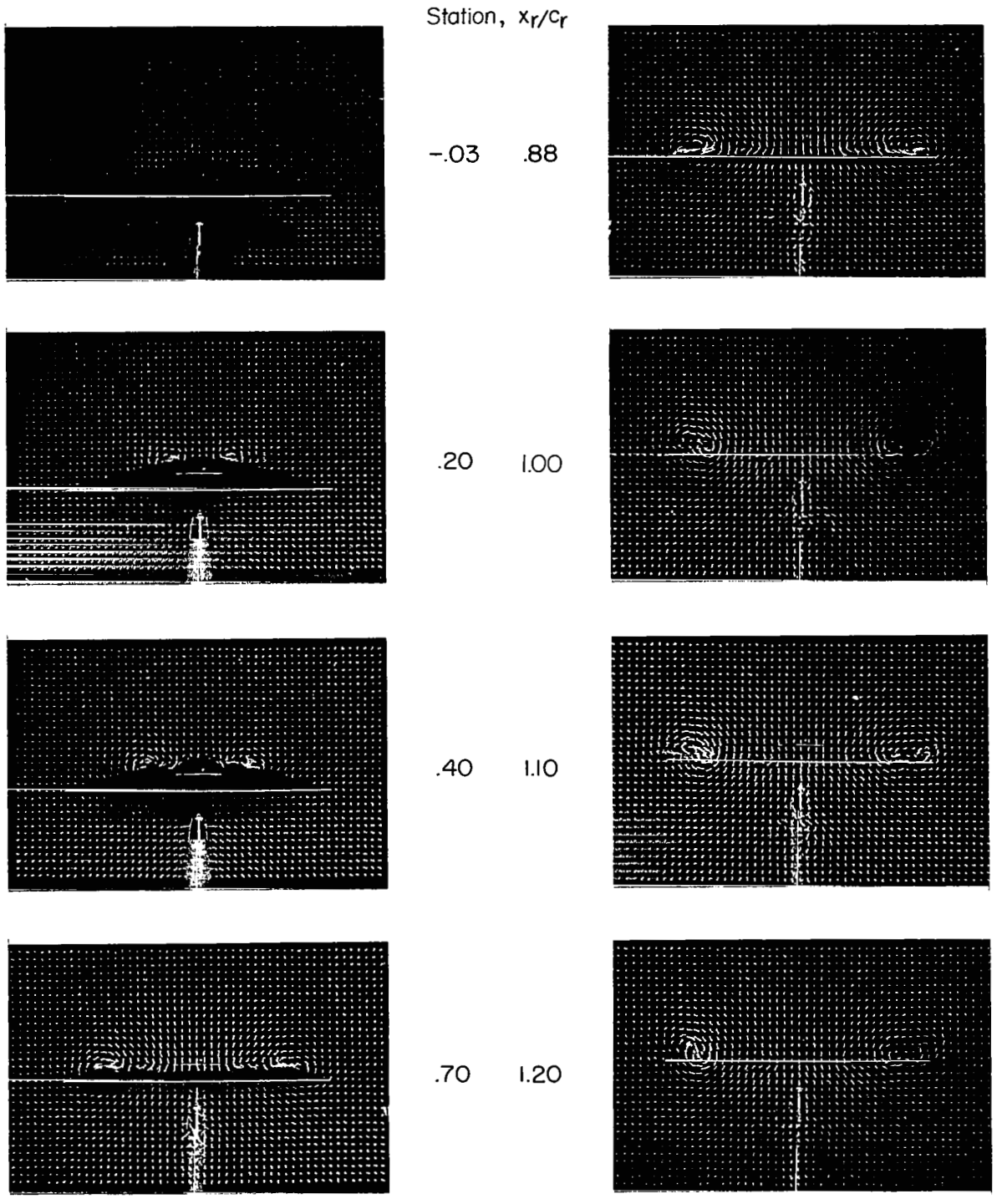

Figure 3.- A tuft-grid survey across the chord of a 60^0 flat-plate delta wing at an angle of attack of 10^0. $\beta = 0^0$. L-68-10,037

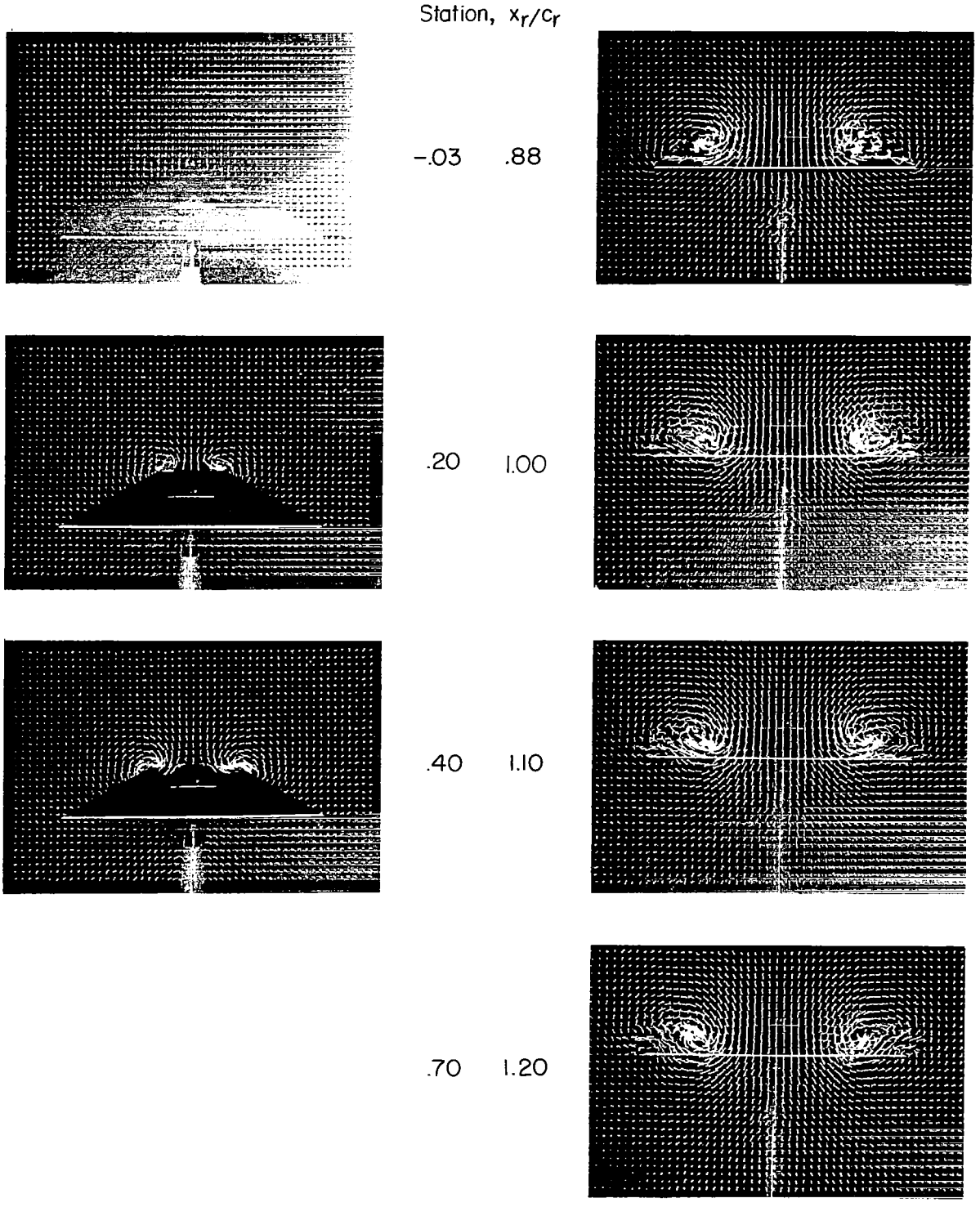

Figure 4.- A tuft-grid survey across the chord of a 60^0 flat-plate delta wing at an angle of attack of 20^0. $\beta = 0^0$. L-68-10,038

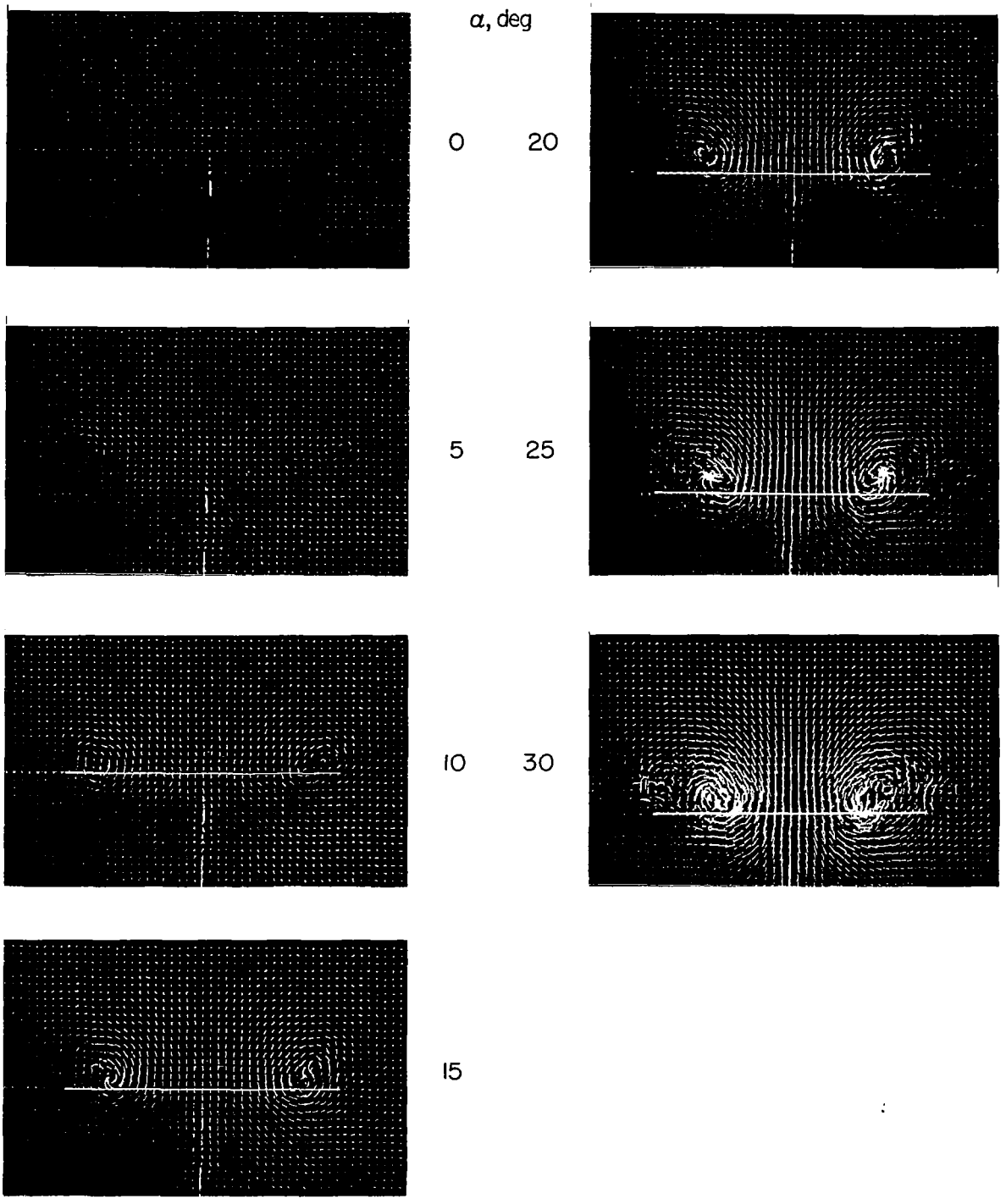

L-68-10,039

Figure 5.- A tuft-grid survey at a location about $0.2c_r$ behind the trailing edge of a 60^0 flat-plate delta wing for a range of angle of attack. $\beta = 0^0$.

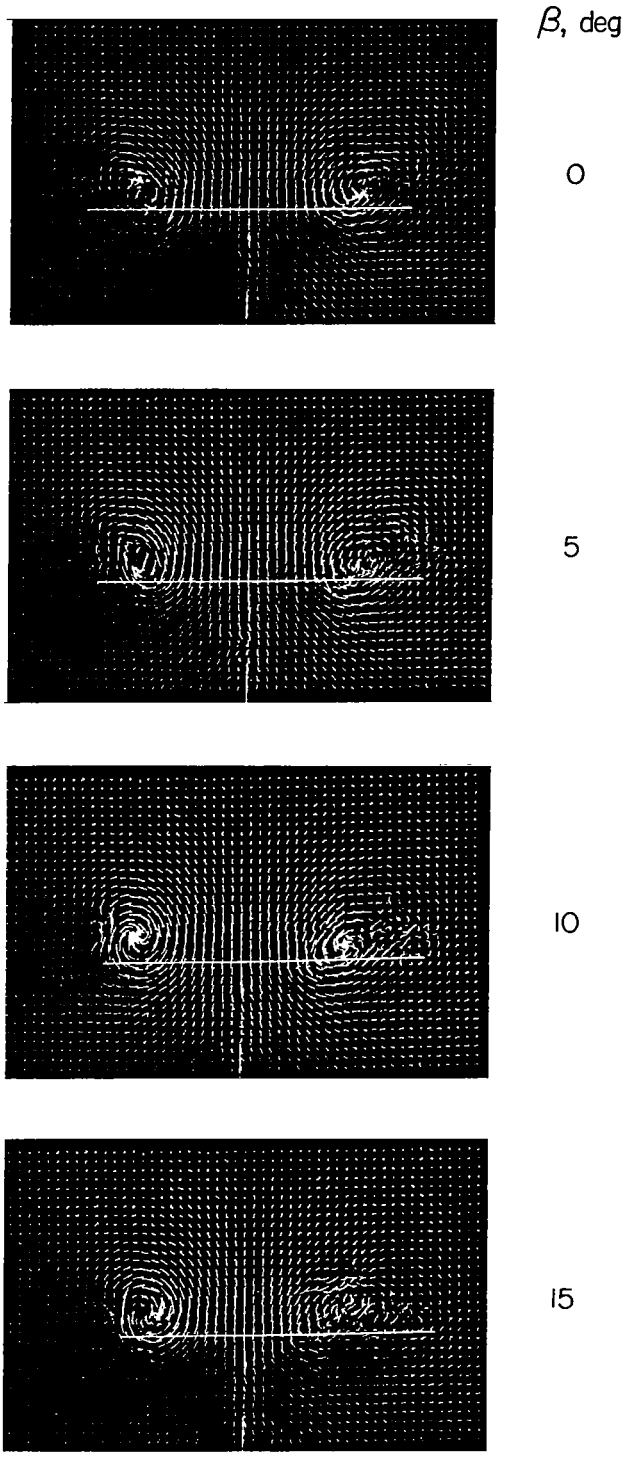

L-68-10,040

Figure 6.- A tuft-grid survey at a location about $0.2c_r$ behind the trailing edge of a 60^0 flat-plate delta wing for a range of slideslip angles. $\alpha = 20^0$.

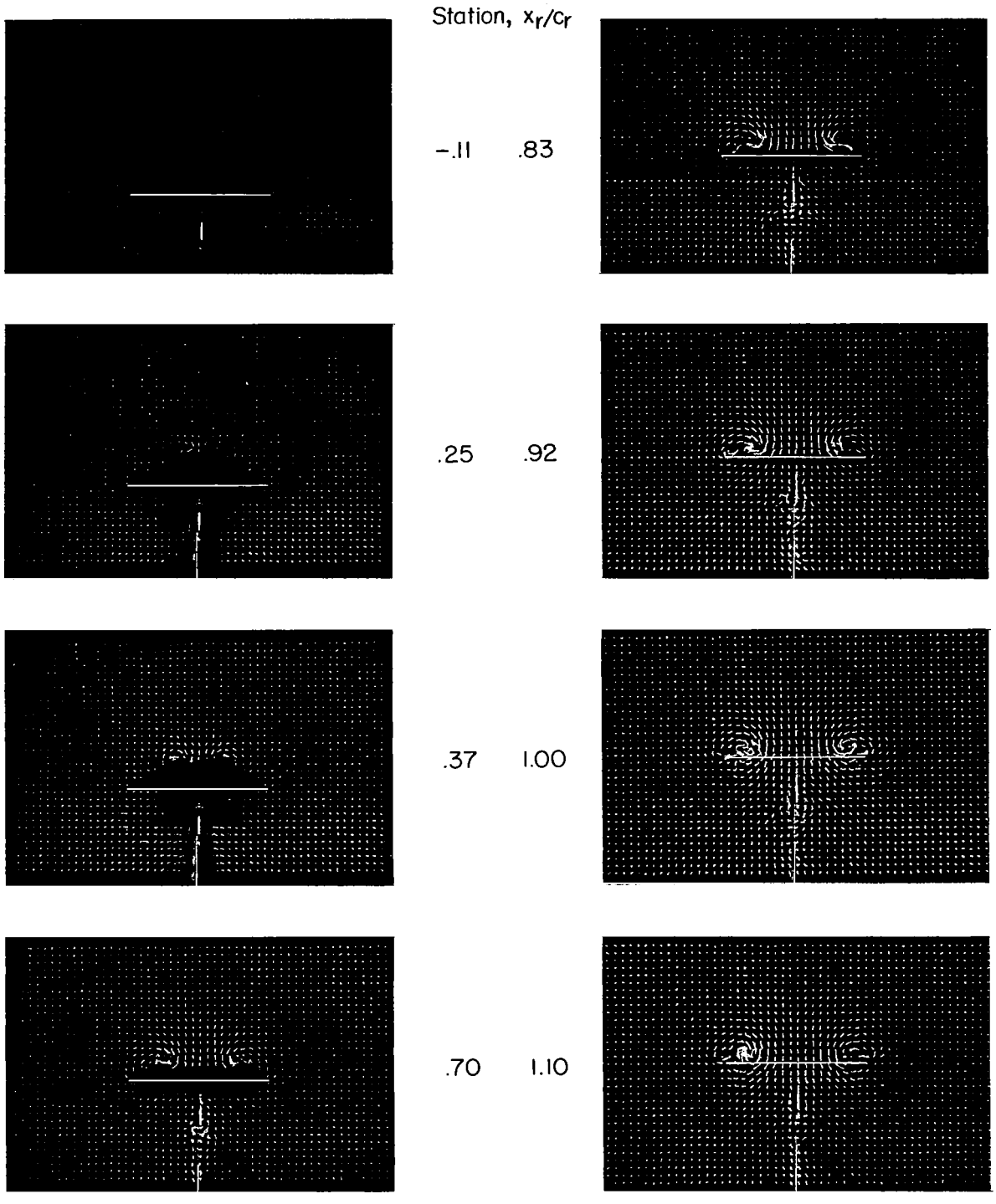

L-68-10,041

Figure 7.- A tuft-grid survey across the chord of a flat-plate delta wing with a 75^0 sweep of the leading edges at an angle of attack of 10^0. $\beta = 0^0$.

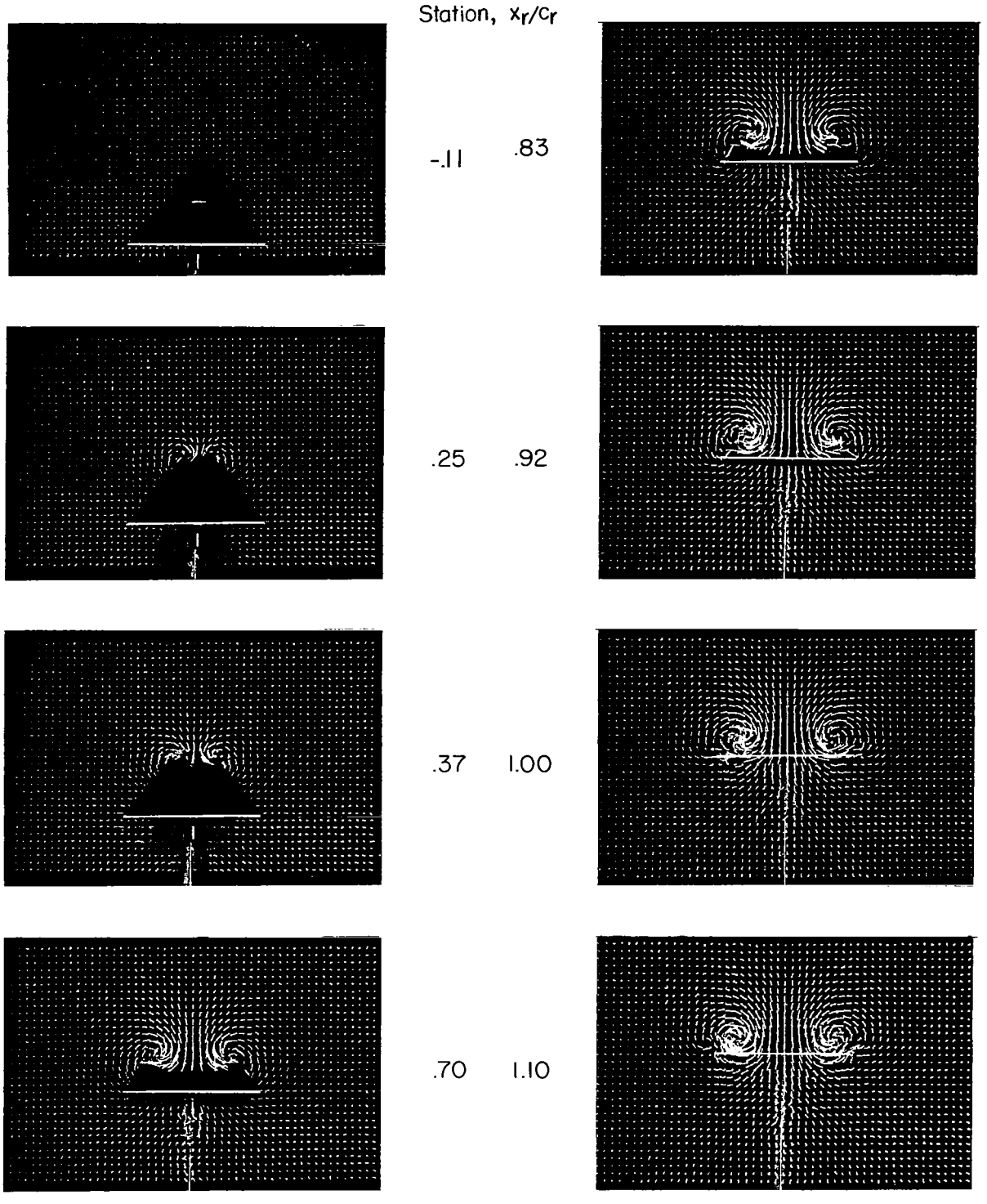

L-68-10,042

Figure 8.- A tuft-grid survey across the chord of a flat-plate delta wing with a 75^0 sweep of the leading edges at an angle of attack of 20^0. $\beta = 0^0$.

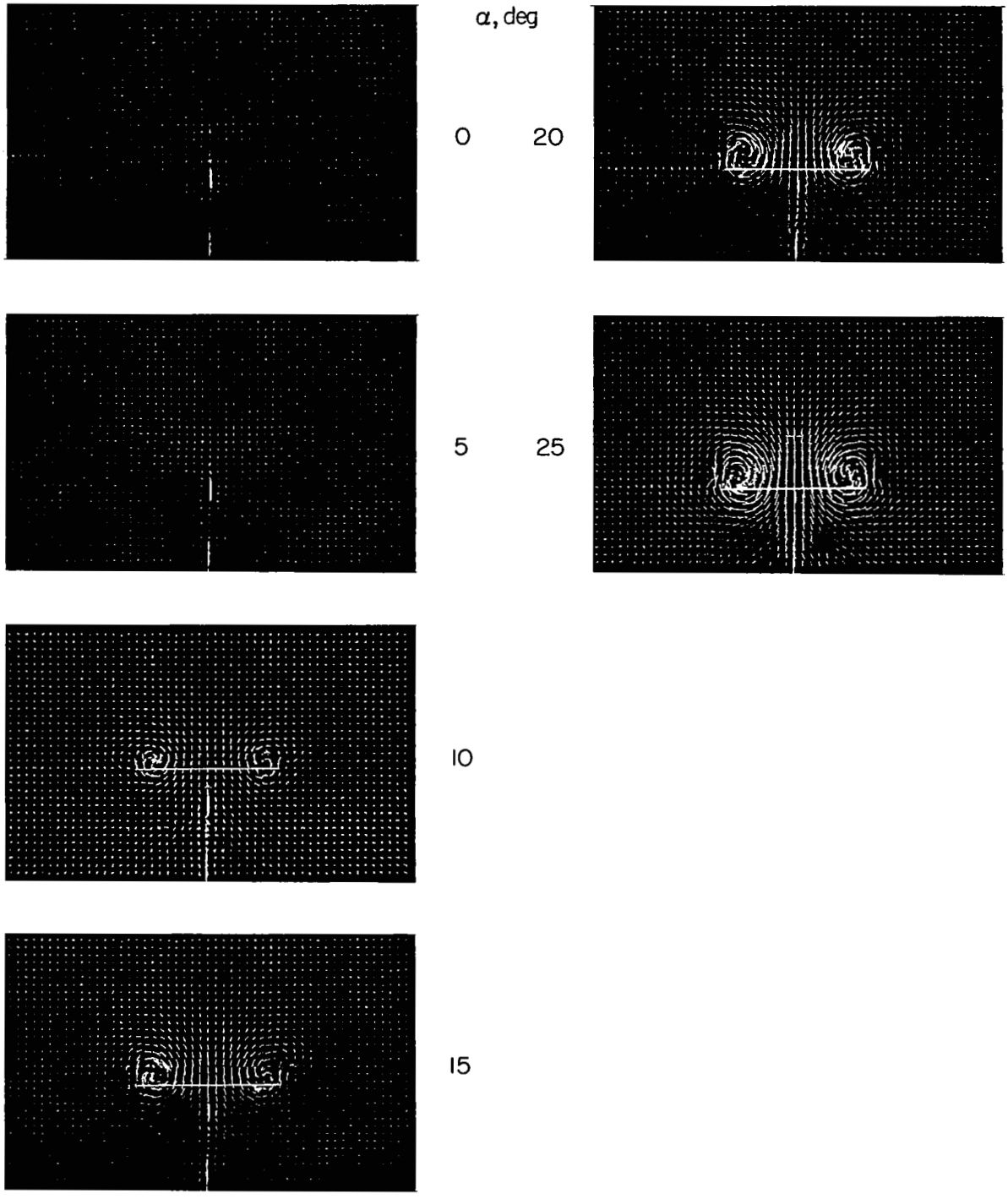

L-68-10,043

Figure 9.- A tuft-grid survey at a location about $0.2c_r$ behind the trailing edge of a flat-plate delta wing with a 75^0 sweep of the leading edges for a range of angle of attack. $\beta = 0^0$.

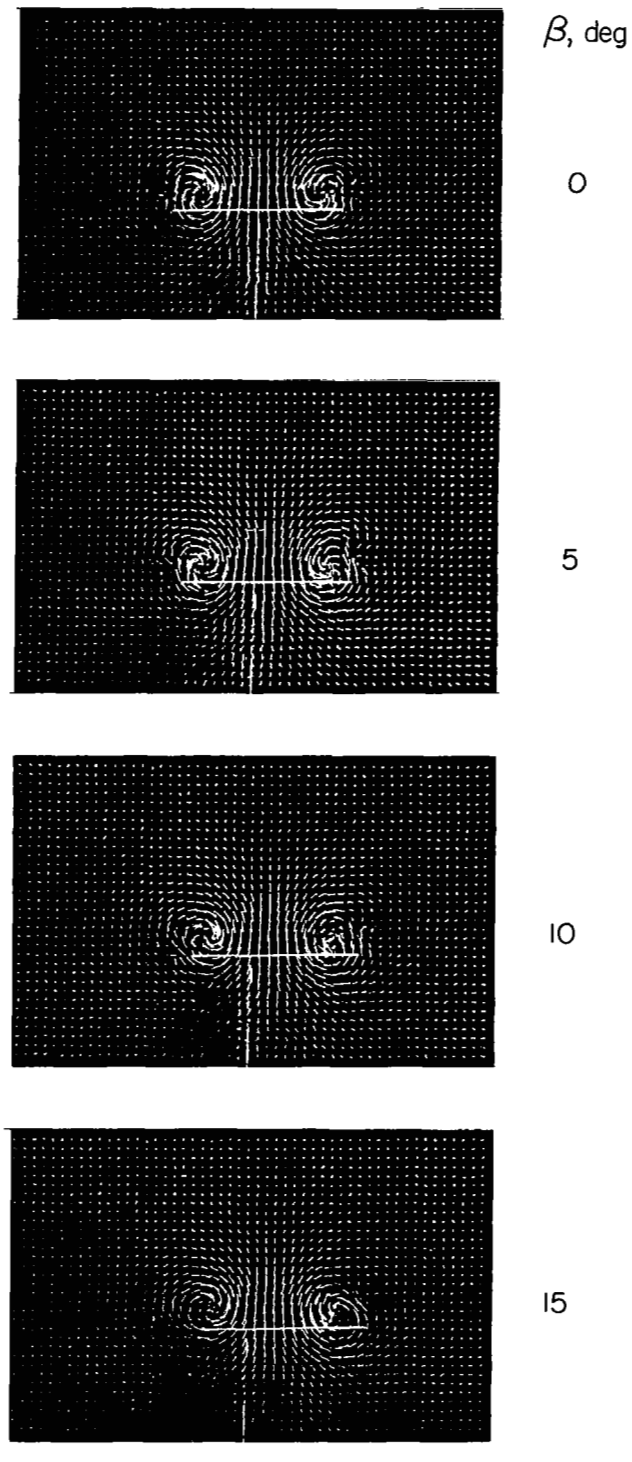

L-68-10,044

Figure 10.- A tuft-grid survey at a location about $0.2c_r$ behind the trailing edge of a flat-plate delta wing with a 75^0 sweep of the leading edges for a range of sideslip angles. $\alpha = 20^0$.

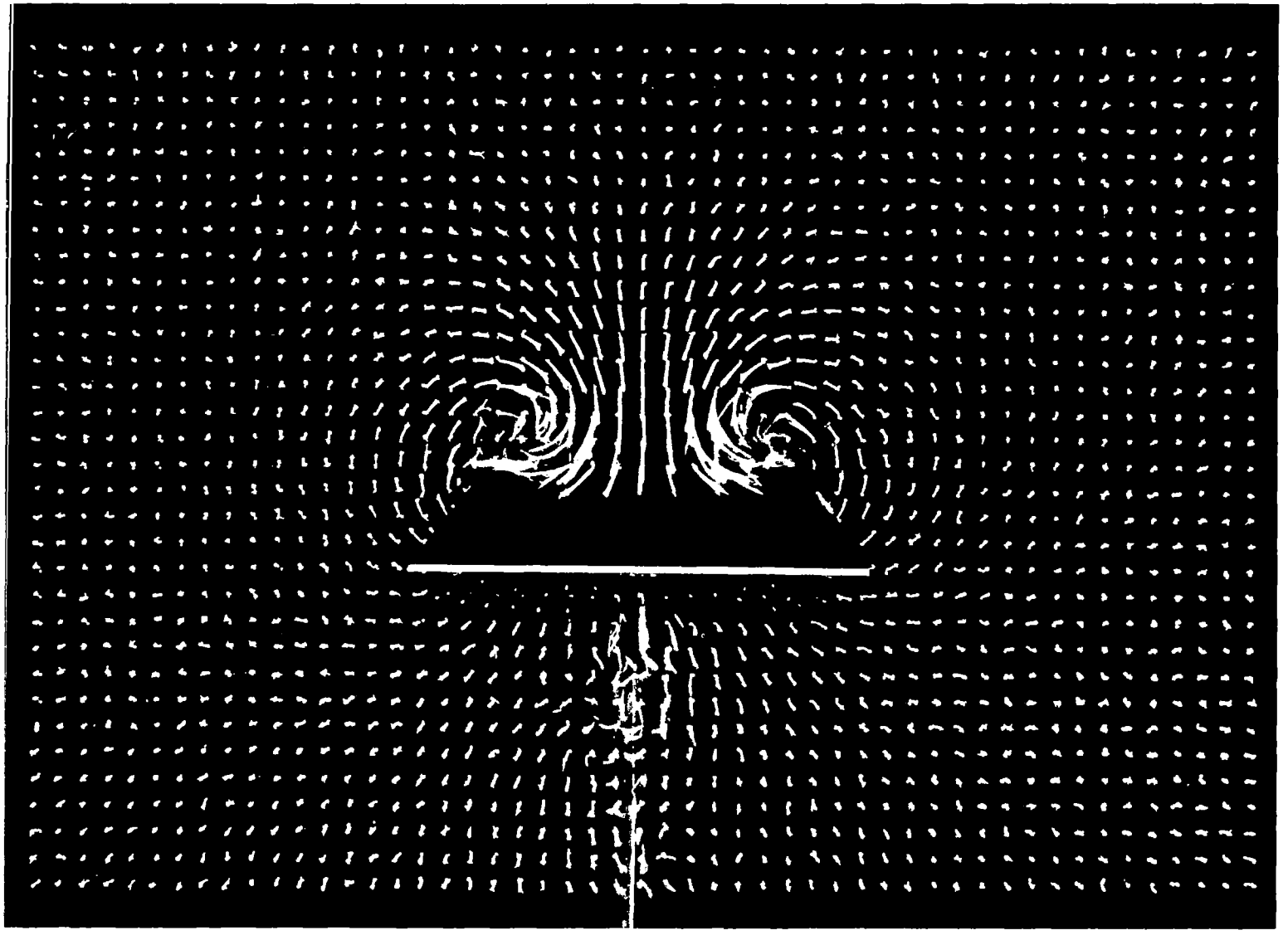

L-68-10,045

Figure 11.- A tuft-grid survey at one chordwise position on a flat-plate delta wing with a 75^{0} sweep of the leading edges (enlargement). $x_r/c_r = 0.70$; $\alpha = 20^{0}$; $\beta = 0^{0}$.

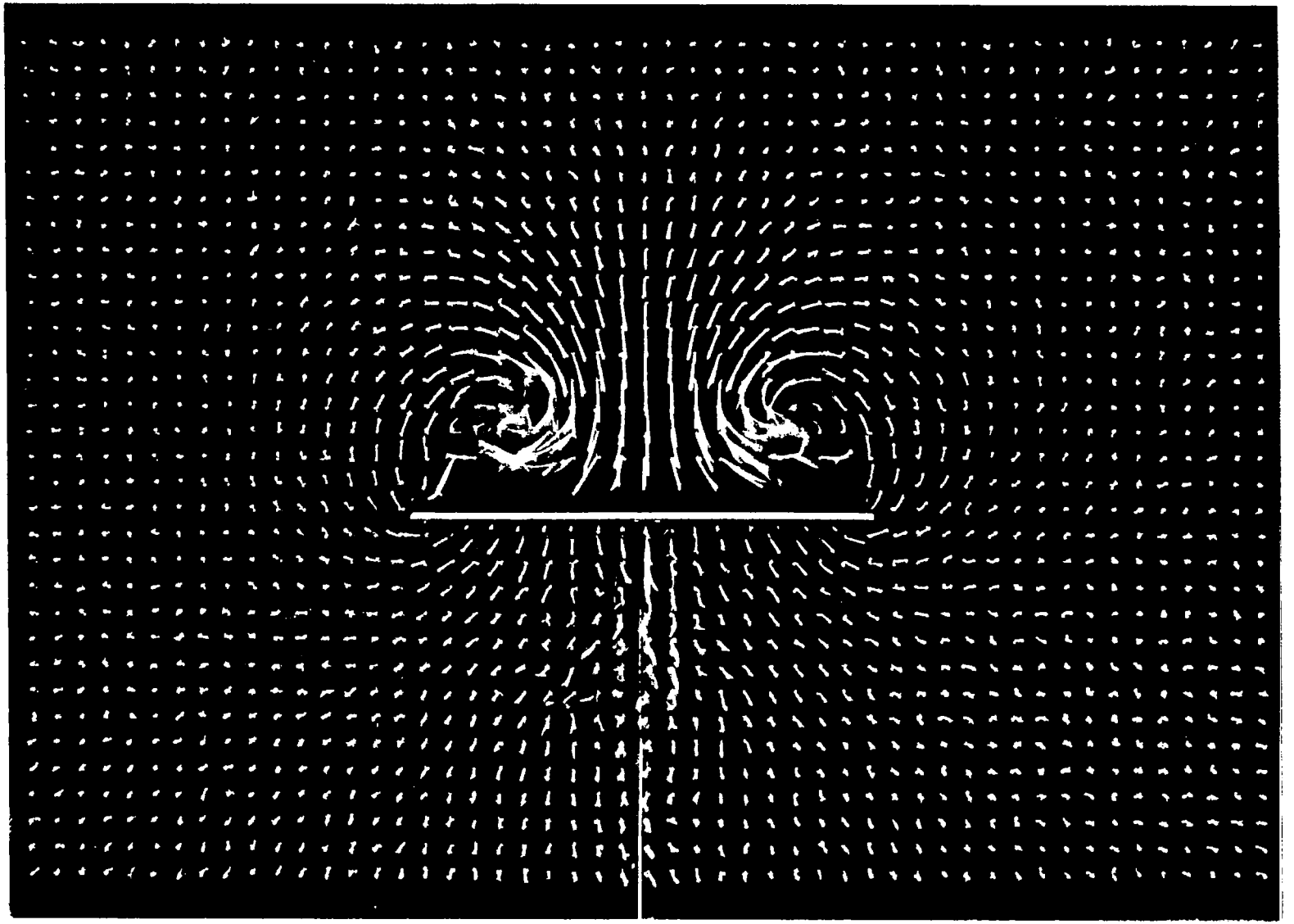

L-68-10,046

Figure 12.- A tuft-grid survey at one chordwise position on a flat-plate delta wing with a 75^0 sweep of the leading edges (enlargement). $x_r/c_r = 0.83$; $\alpha = 20^0$; $\beta = 0^0$.

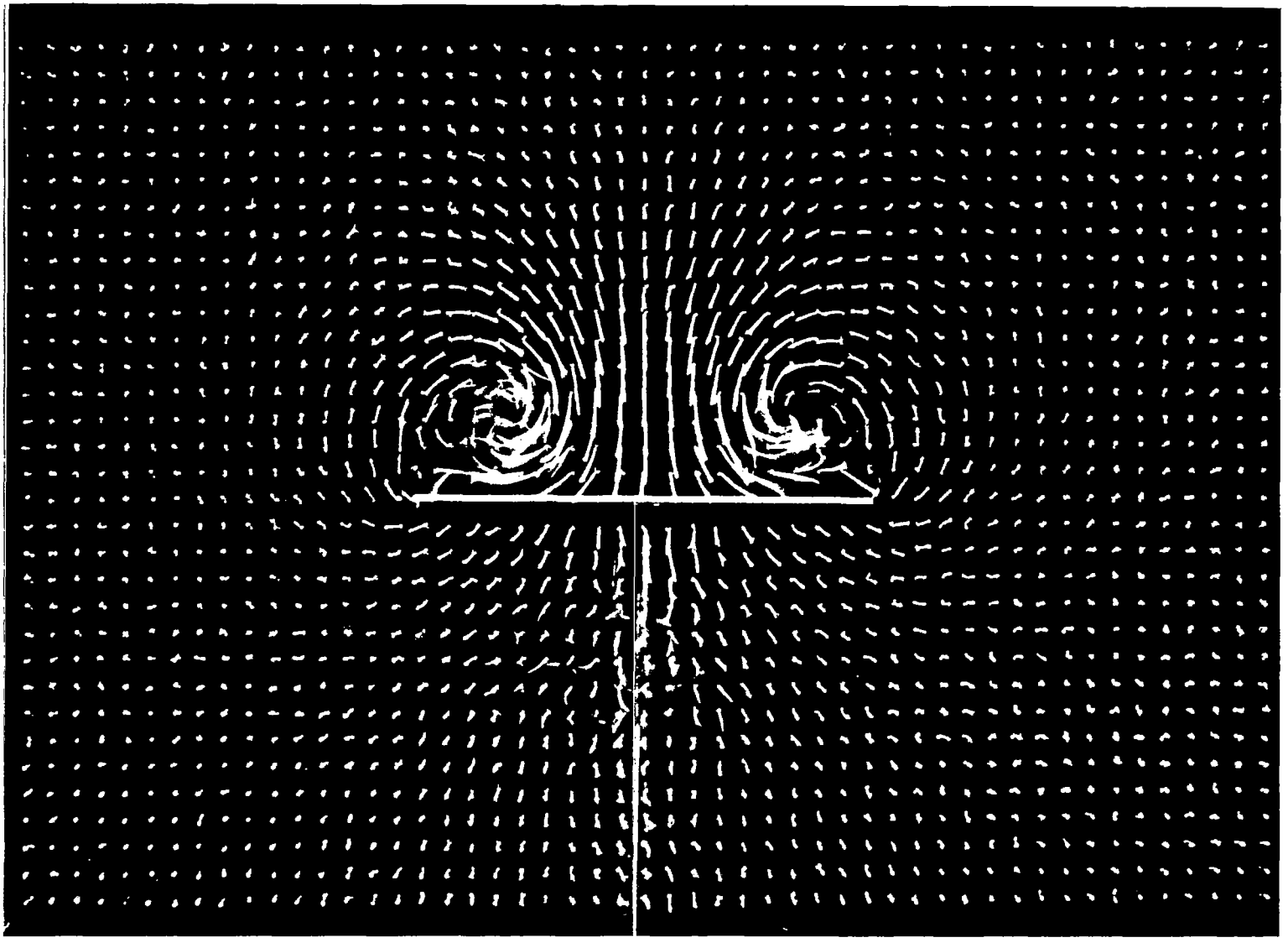

L-68-10,047

Figure 13.- A tuft-grid survey at one chordwise position on a flat-plate delta wing with a 75^0 sweep of the leading edges (enlargement). $x_r/c_r = 0.92$; $\alpha = 20^0$; $\beta = 0^0$.

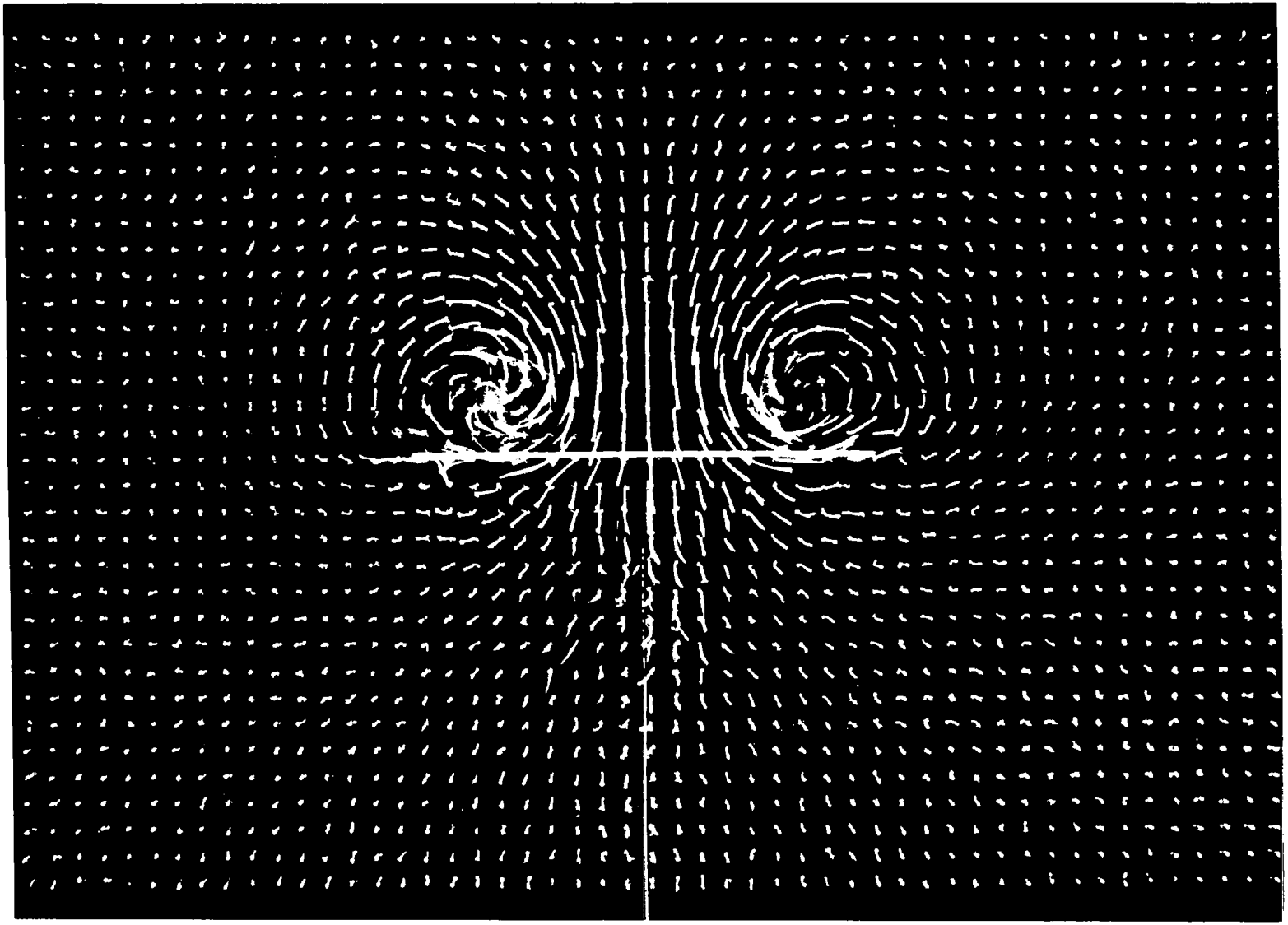

L-68-10,048

Figure 14.- A tuft-grid survey at one chordwise position on a flat-plate delta wing with a 75^0 sweep of the leading edges (enlargement). $x_r/c_r = 1.00$; $\alpha = 20^0$; $\beta = 0^0$.

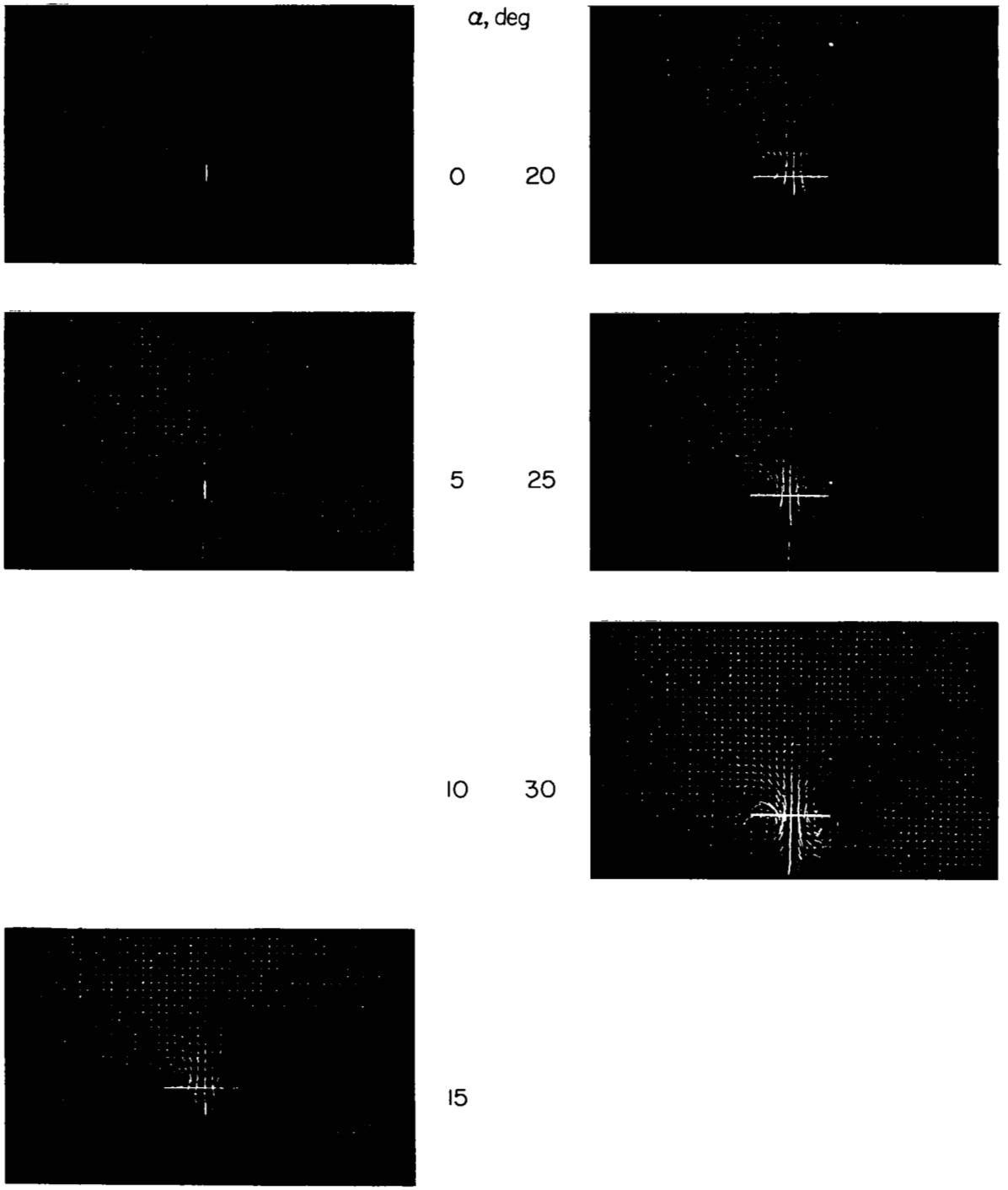

L-68-10,049

Figure 15.- A tuft-grid survey at a location about $0.2c_r$ behind the trailing edge of a flat-plate delta wing with an 82.5^0 sweep of the leading edges for a range of angle of attack. $\beta = 0^0$.

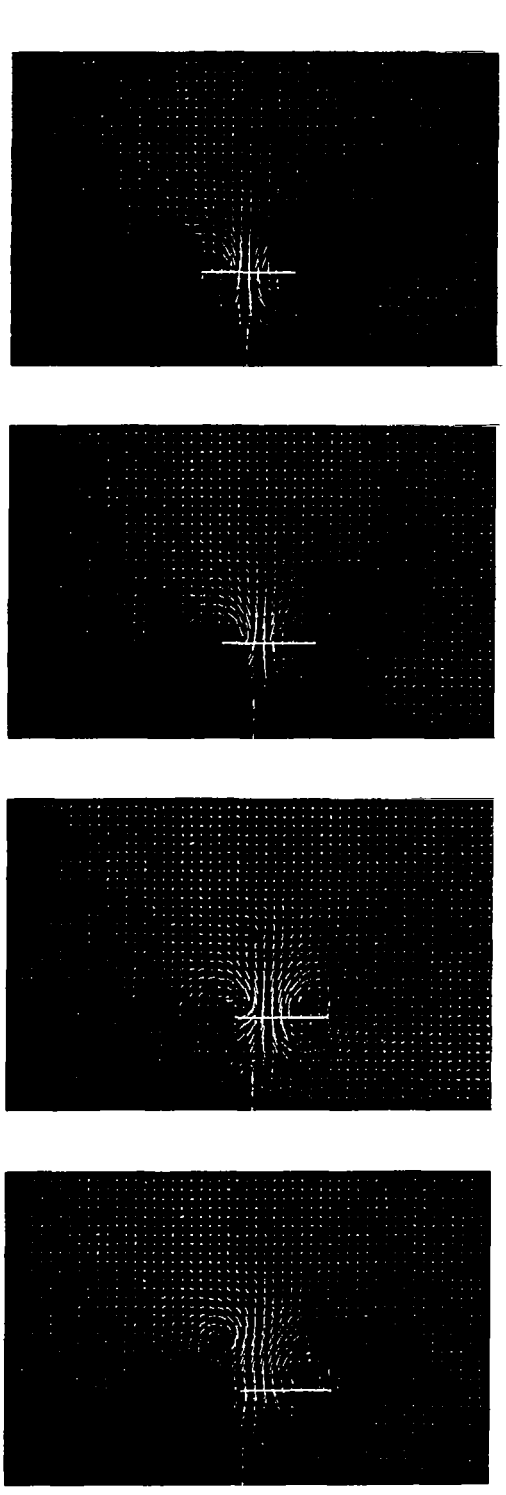

L-68-10,050

Figure 16.- A tuft-grid survey at a location about $0.2c_r$ behind the trailing edge of a flat-plate delta wing with an 82.5^0 sweep of the leading edges for a range of sideslip angles. $\alpha = 25^0$.

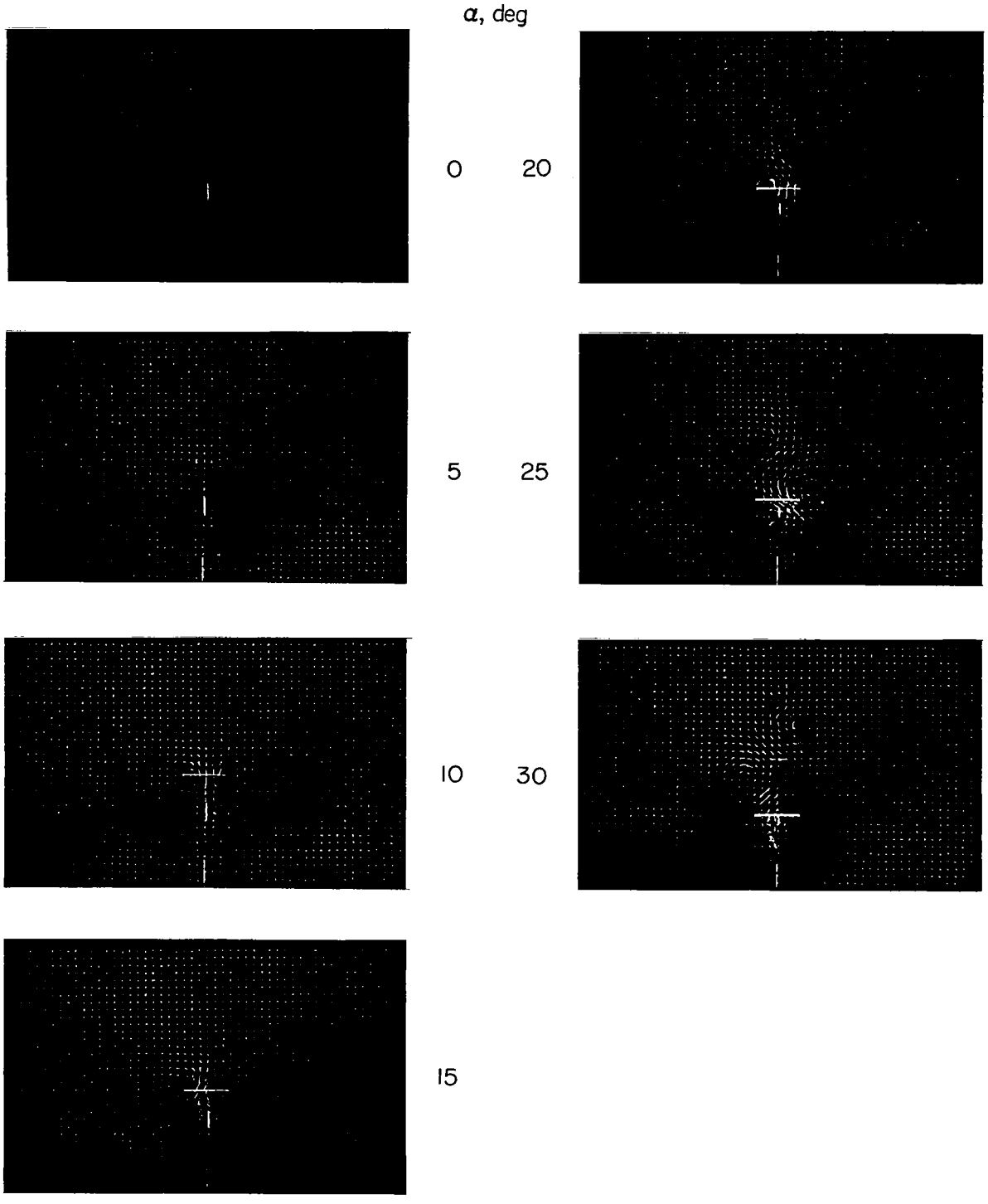

L-68-10,051

Figure 17.- A tuft-grid survey at a location about $0.2c_r$ behind the trailing edge of a flat-plate delta wing with an 86.5^0 sweep of the leading edges for a range of angle of attack. $\beta = 0^0$.

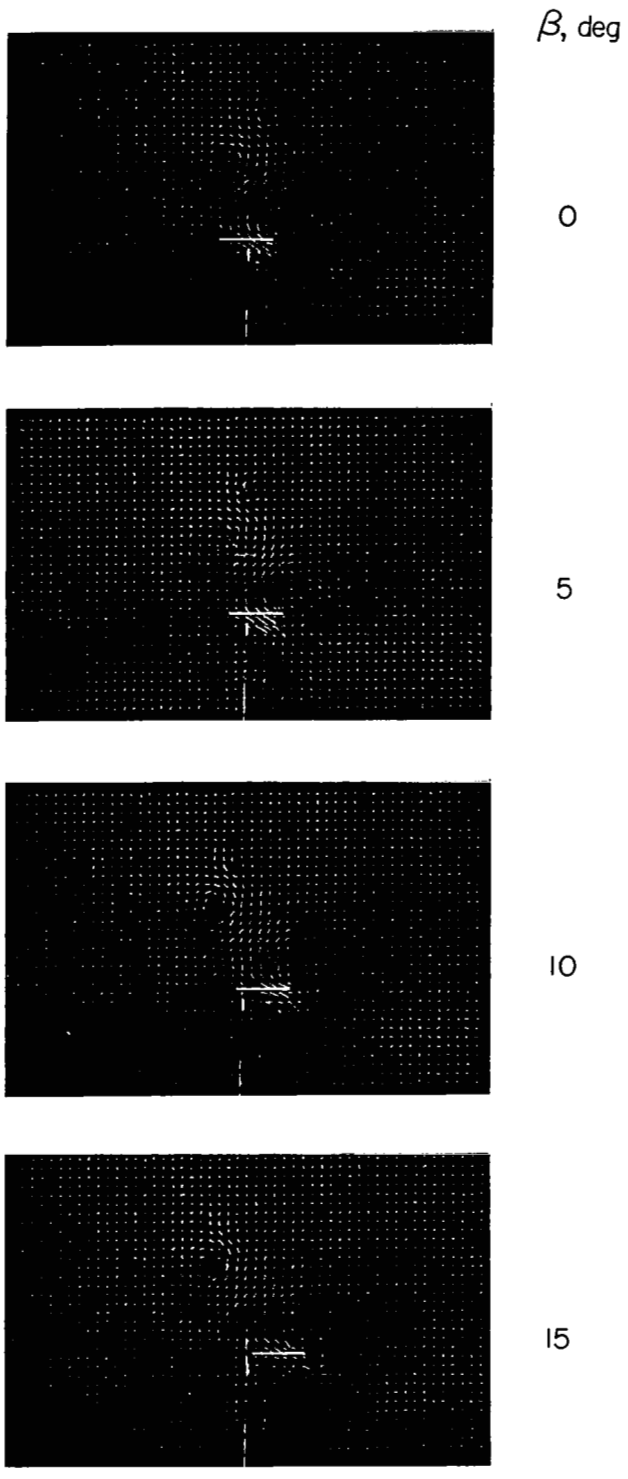

L-68-10,052

Figure 18.- A tuft-grid survey at a location about $0.2c_r$ behind the trailing edge of a flat-plate delta wing with an 86.5^0 sweep of the leading edges for a range of sideslip angles. $\alpha = 25^0$.

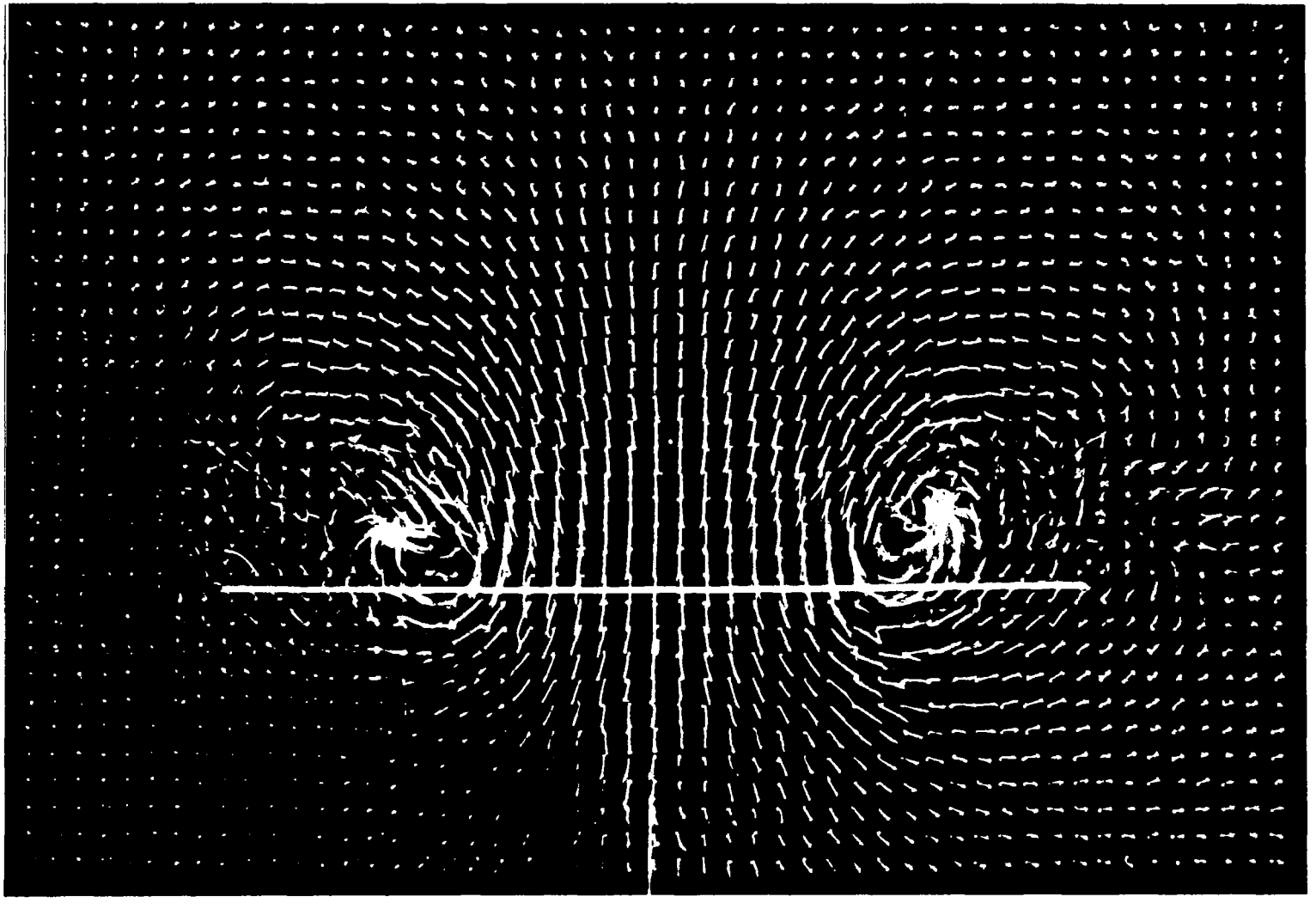

L-68-10,053

Figure 19.- A tuft-grid survey at about $0.2c_r$ behind the trailing edge of a flat-plate delta wing with a 60^0 sweep of the leading edges for $\alpha = 25^0$ and $\beta = 0^0$.

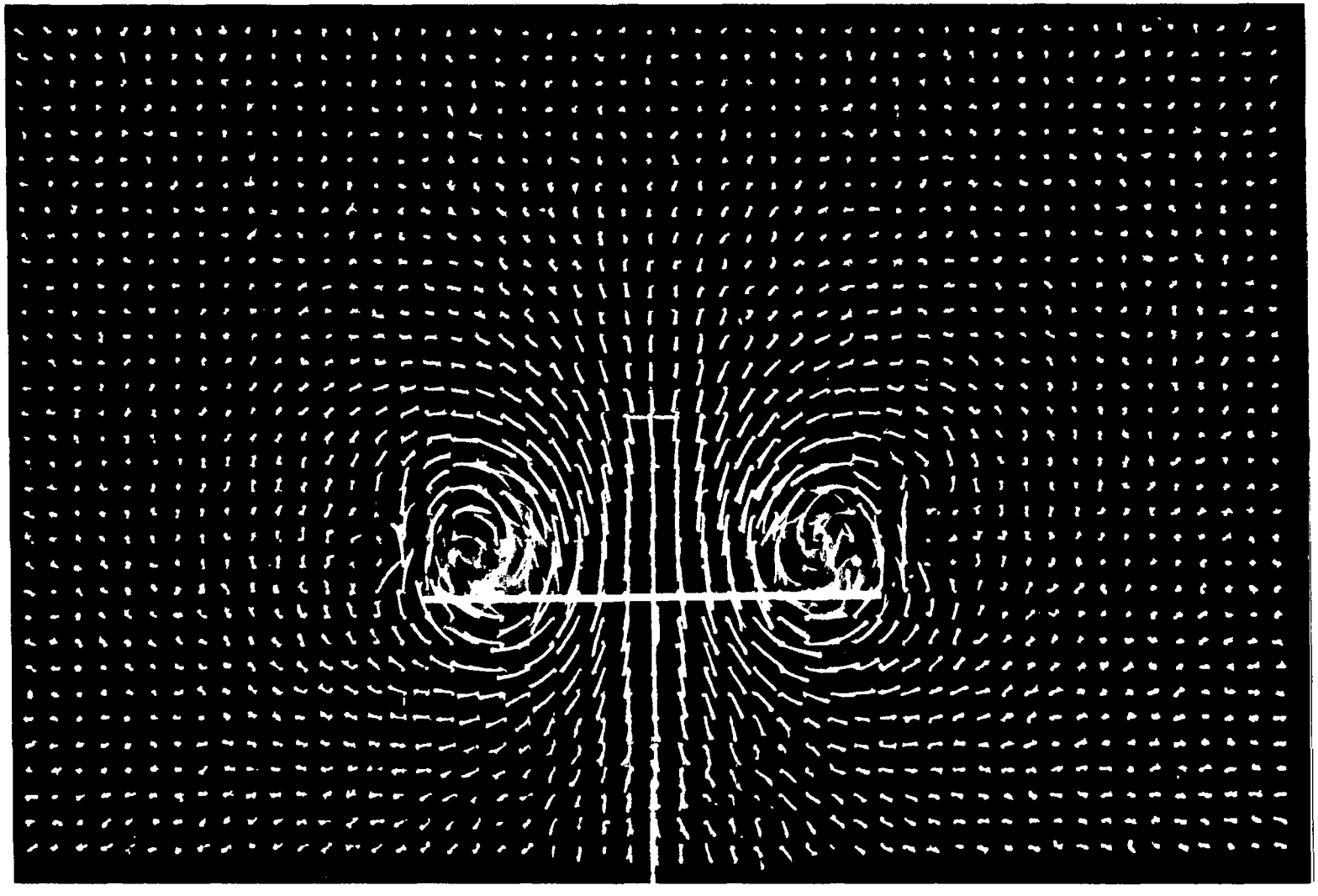

L-68-10,054

Figure 20.- A tuft-grid survey at about $0.2c_r$ behind the trailing edge of a flat-plate delta wing with a 75^0 sweep of the leading edges for $\alpha = 25^0$ and $\beta = 0^0$.

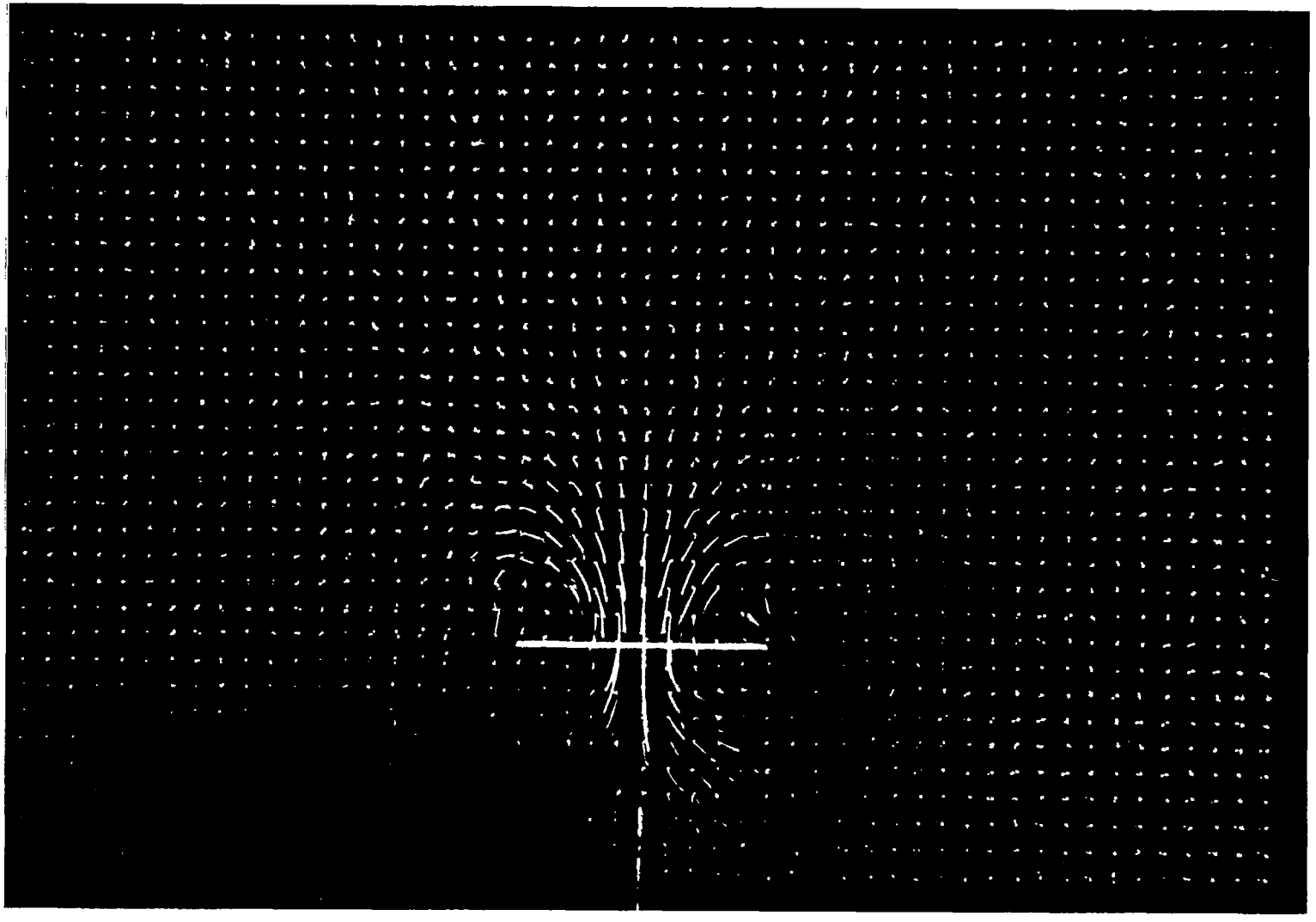

L-68-10,055

Figure 21.- A tuft-grid survey at about $0.2c_r$ behind the trailing edge of a flat-plate delta wing with an 82.5^0 sweep of the leading edges for $\alpha = 25^0$ and $\beta = 0^0$.

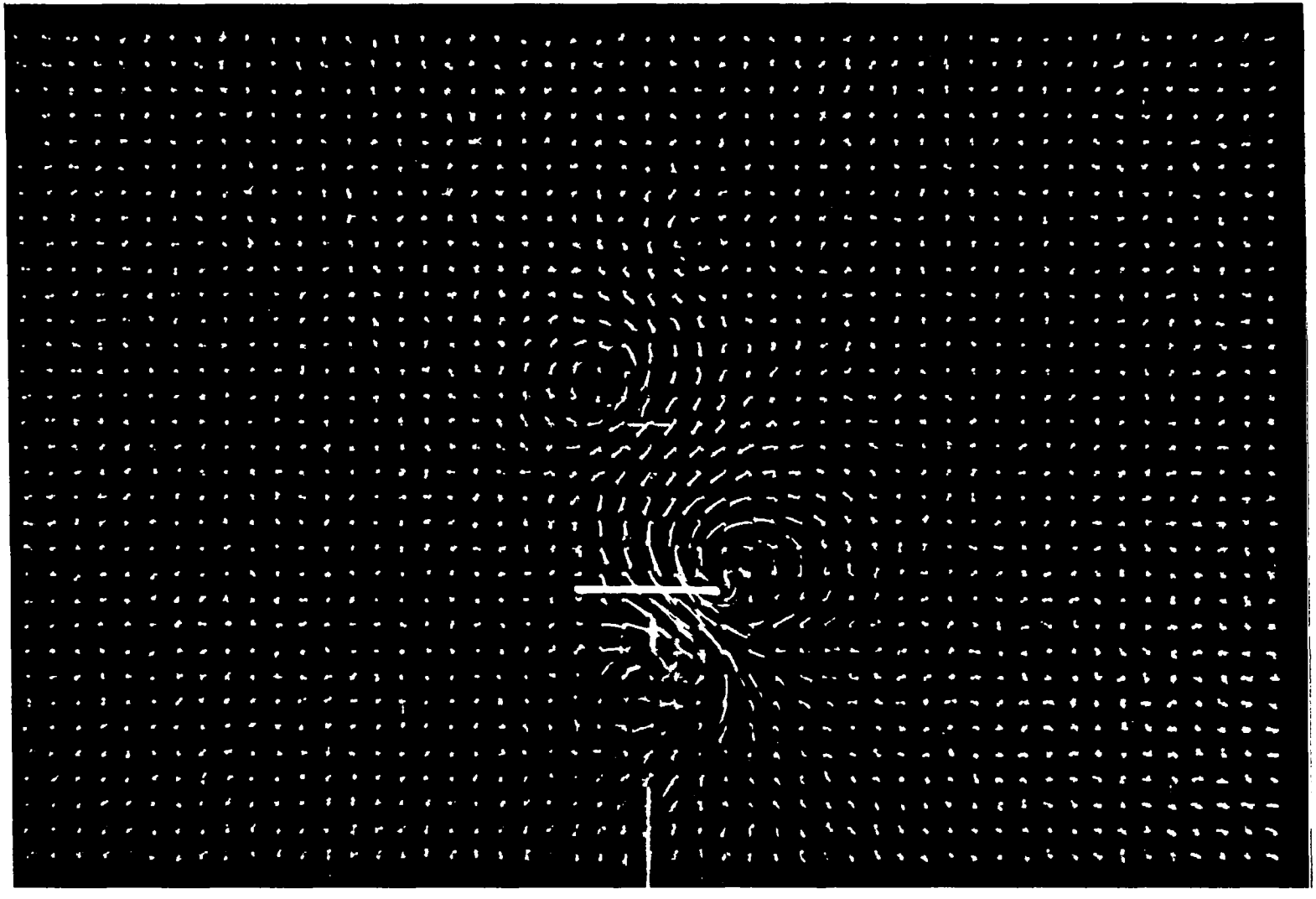

L-68-10,056

Figure 22.- A tuft-grid survey at about $0.2c_r$ behind the trailing edge of a flat-plate delta wing with an 86.5^0 sweep of the leading edges for $\alpha = 25^0$ and $\beta = 0^0$.

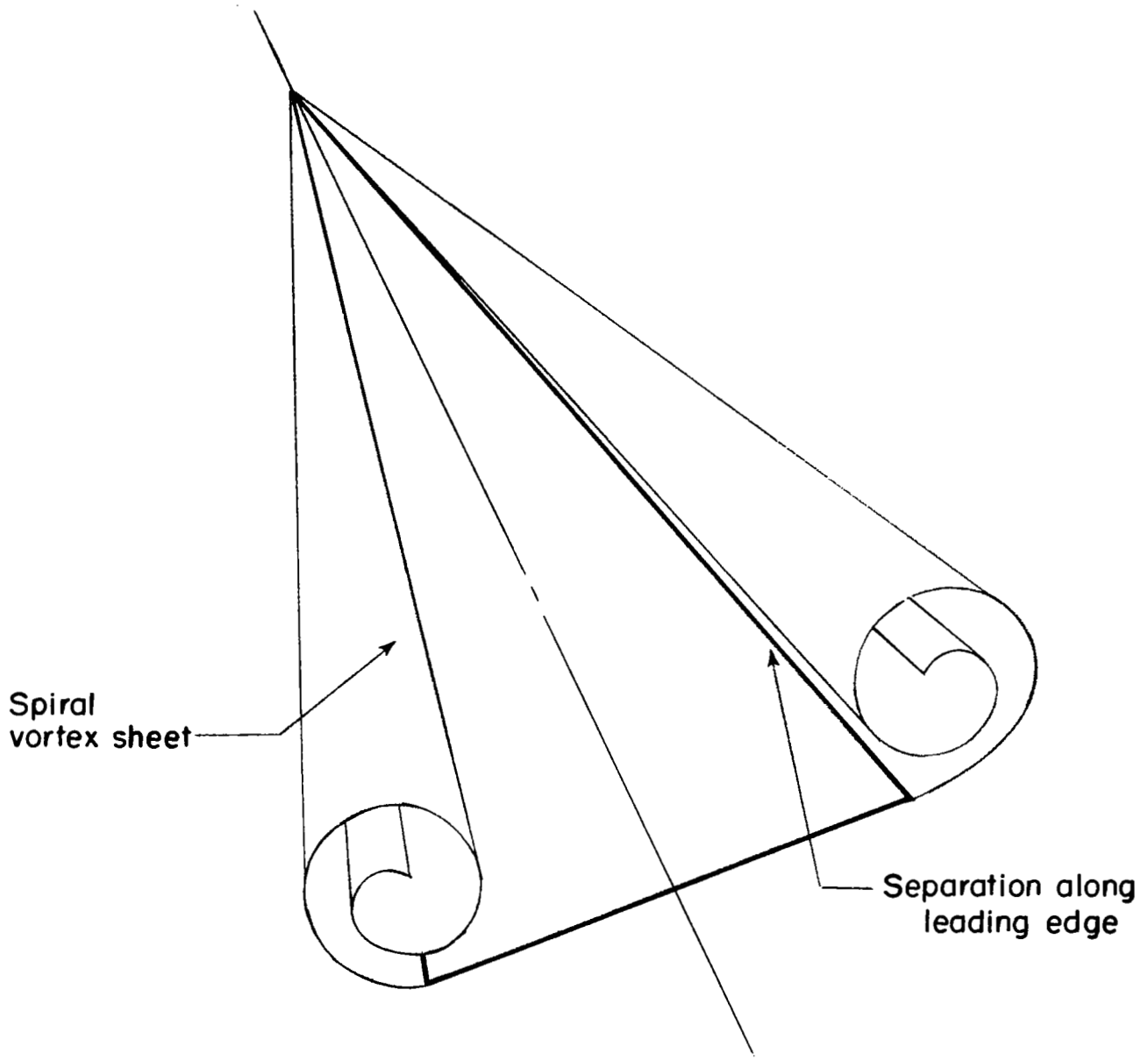

Figure 23.- Illustration of vortex flow.